Polarization selective spectroscopy experiments: methodology and pitfalls

Howe-Siang Tan,* Ivan R. Piletic, and M. D. Fayer

Department of Chemistry, Stanford University, Stanford, California 94305

Received February 14, 2005; revised manuscript received April 6, 2005; accepted April 6, 2005

We analyze the effectiveness of various practical implementations of time-dependent pump–probe and transient grating polarization-selective experiments. A variety of optical arrangements are analyzed in the Jones matrix calculus framework. The optical arrangements that permit the correct determination of the time-dependent orientational and excited-state population dynamics are delineated. It is shown that magic angle transient grating experiments yield pure population dynamics under certain conditions only. The effectiveness of spectrally resolved magic angle pump–probe and transient grating experiments that use a monochromator are shown to be dependent on the position of an analyzing polarizer along the experimental beam path relative to various other optical elements. The spectrally resolved experiments will measure pure population dynamics only if a polarizer is placed immediately after the sample. The effectiveness of experiments measuring orientational dynamics by separately measuring the probe signal with its polarization parallel and perpendicular to the pump polarization is not constrained by the conditions imposed on the magic angle experiments.

OCIS codes: 320.7150, 320.7100.

1. INTRODUCTION

The use of polarization-selective techniques is common in many time-resolved optical spectroscopy experiments. These include pump–probe anisotropy experiments to study orientational dynamics of molecular systems.[1–3] Transient grating experiments, related in nature to pump–probe experiments, are also used for such studies.[4–6] Experiments, both pump–probe and transient grating, that recover excited-state population lifetime dynamics independently of orientational relaxation contributions are also routinely performed in a so-called magic angle configuration.[1,2,7] These experiments have in common the careful manipulation of the polarizations of the interacting optical pulses and polarization-selective detection of the signal. The theoretical aspects of polarization experiments are well developed and chronicled.[2,8,9] However, the theoretical studies do not take into account the many complications that arise from the practical implementations of the detection schemes. Optical elements, for example, simple metallic mirrors, polarizers, wave plates, and diffraction gratings, need to be placed along the path of the light beams. These optical elements inevitably affect the polarization of the light beams involved in the experiments.

Until recently, the bulk of polarization spectroscopy experiments had been performed in the visible or UV spectral region to study electronic transitions. It is only recently, with the development and refinement of intense infrared ultrafast laser sources, that similar polarization experiments have been performed on molecular vibrations. Ultrafast spectroscopy of vibrational systems has to take into consideration the 0–1 as well as the 1–2 vibrational transition. Hence frequency resolving the signal with a monochromator before detection is often done to separate the 0–1 and 1–2 transition contributions.[10–14] Spectrally resolved pump–probe experiments are also useful in the visible–UV to isolate the signal from a particular species. The addition of a monochromator results in certain somewhat subtle issues of what is actually being observed in a given experiment. For instance, diffraction gratings in monochromators affect the polarization of the light fields. The placement of polarizers along the optical path relative to other optical elements alters the final measurement of the signal.

Although the literature on the theoretical aspects of polarization spectroscopy is rich, literature regarding the consistent practical implementation of these experiments is lacking. In this paper we use the Jones matrix formulism[15,16] to analyze some relevant optical setups for polarization-selective spectroscopy. The Jones matrix formalism has been used to analyze linear and circular dichroism spectroscopy[17,18] and optical Kerr effect experiments.[19] We use a similar approach and consider the effect of other polarization-selective optical elements on the experimental observables. It is shown that frequently the simplest implementation of polarization spectroscopy can lead to erroneous results. In Section 2 we describe the Jones matrices for the optical elements and the signal generation and detection that are relevant for various experiments. In Section 3 we analyze the signals measured in a magic angle configuration in pump–probe and transient grating experiments in various experimental setups. In Section 4 we consider experiments that measure orientational anisotropy decay. We summarize the results of our analysis in Section 5.

2. FORMALISM

The Jones matrix calculus[15,16] is a useful representation for the mathematical manipulation of polarized light. A light field E_i propagating along the z axis can be written as

$$\vec{E}_i(\theta_i) = A_i \exp(-i\omega t)[\hat{x} \exp(i\phi)\cos\theta_i + \hat{y} \sin\theta_i], \quad (1)$$

where A_i is the complex amplitude of the light field, $\hat{x}$ and $\hat{y}$ are unit vectors that represent the light-field polarization direction, θ_i is the angle of polarization of the light field from the x axis, and ϕ denotes the relative phase shift between the two polarization components. The light field as described in Eq. (1) can also be represented by a vector with polarization-direction unit vectors $\hat{x}$ and $\hat{y}$ as the basis set:

$$\vec{E}_i(\theta_i) = \begin{bmatrix} \exp(i\phi)\cos\theta_i \\ \sin\theta_i \end{bmatrix}. \quad (2)$$

For brevity we have suppressed the oscillatory term $\exp(-i\omega t)$ in Eq. (2). Amplitude term A_i is also omitted because we are interested only in the relative amplitudes of the polarization components rather than in the absolute amplitudes. Without any loss of generality we define the direction along the x axis as the direction of the polarization of the pump pulse(s) in the pump–probe and transient grating experiments. The x-axis and y-axis directions are termed parallel ($\parallel$) and perpendicular ($\perp$), respectively. Another common convention can be used when we consider the reflection or diffraction from surfaces. S and P polarization, respectively, represent the polarization perpendicular and parallel to the plane of incident and reflection (or diffraction). On an optical table, mirrors and gratings are usually placed in such as way that the surfaces are perpendicular to the laser table. In this case, assuming that the polarization of the pump pulse(s) is parallel to the laser table, the x axis and the parallel ($\parallel$) axis correspond to P polarization and the y axis and the perpendicular ($\perp$) axis correspond to S polarization. These are the conventions that are used for this paper, and they are depicted in Fig. 1.

In the Jones matrix calculus, optical elements such as polarizers, wave plates, and mirrors are represented by operator matrices. These operator matrices transform the light-field vectors in the same manner that the optical elements transform the light fields' polarization.

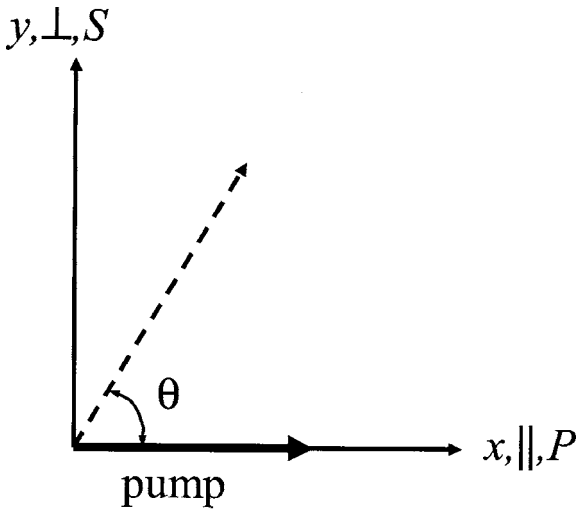

Fig. 1. Axis system and conventions used to describe the pump- and probe-pulse polarization. The propagation direction is along the z axis. The polarization of the pump pulse(s) is along the x axis, which is also termed the parallel ($\parallel$) axis. Angle θ of the probe-beam polarization or polarizer settings is referenced from the x axis.

Polarizers are used extensively in polarization-selective experiments. The matrix operator for a polarizer set at angle θ from the x–z plane (Fig. 1) can be described by

$$\mathbf{P}(\theta) = \begin{bmatrix} \cos^2\theta & \cos\theta\sin\theta \\ \cos\theta\sin\theta & \sin^2\theta \end{bmatrix}. \quad (3)$$

Metallic mirrors are a mainstay of optical experiments. Metallic mirrors are not ideal reflectors. On reflection, S and P polarization, in general, acquire different phase shifts.[20] The relative phase shift δ between S and P polarization can be considerable. For a single reflection from a silver mirror at 45° incident angle, this value is estimated to be 2.6° and 26° at 5 μm and 500 nm, respectively.[21] Furthermore, commercially available metallic mirrors often come with dielectric or oxide coatings over the metal surfaces for protective and reflection-enhancing purposes. Such coatings contribute to the phase-shift difference between S and P polarization. Relative phase shift δ that is imparted to the light field by reflecting or diffracting from a metallic surface is described by the matrix operator

$$\mathbf{M} = \begin{bmatrix} \exp(i\delta) & 0 \\ 0 & 1 \end{bmatrix}. \quad (4)$$

In general, for a linearly polarized light field impinging upon a metal mirror surface the reflected light will be elliptical if the incident polarization is not strictly S or P. Here we are taking the reflectivity for S and P polarization to be identical. In practice, the reflectivities are quite similar but not identical. (For a silver mirror at 500 nm with a 45° incident angle the reflectivities are ~98% and ~96% for S and P polarization, respectively; there is negligible difference at 5 μm). The influence of the difference in reflectivity is discussed below.

Polarization-selective optics are defined here as optical elements that have a different transmittance or reflectance for different polarizations of the incident light field. For example, a diffraction grating has a diffraction efficiency that depends on whether the incident light is P or S polarized.[22] For instance, a 120 groove/mm diffraction grating blazed for 4 μm wavelength light has a 1.5 times better diffraction efficiency for P polarization than for S polarization for 4 μm light. The effect of the difference in efficiency is represented by

$$\mathbf{T} = \begin{bmatrix} \alpha & 0 \\ 0 & \beta \end{bmatrix}, \quad (5)$$

where α^2 and β^2 are, respectively, the efficiencies of transmittance–reflectance for the parallel and perpendicular components of the light fields at the intensity level. This operator can also be applied to other polarization-selective optics such as beam splitters.

Interaction of the light field with the sample under study can be treated within the framework of diagrammatic perturbation theory. In this context, pump–probe and transient grating spectroscopies are similar experiments that can be described in terms of third-order nonlinear polarization processes.[23] In a transient grating ex-

periment, two pump pulses with directional vectors $\mathbf{k}_1$ and $\mathbf{k}_2$ that are coincident in time interact with the sample. After a delay τ, a third pulse, in the direction $\mathbf{k}_3$, interacts with the sample and creates a signal light field that propagates in the $\mathbf{k}_s=-\mathbf{k}_1+\mathbf{k}_2+\mathbf{k}_3$ direction. In a more physically intuitive description, the two pump pulses produce an optical interference pattern that excites the sample with a spatial distribution of excitation that mimics the interference pattern. Where there is excitation (fringe peaks), the sample's optical susceptibility is different from that at positions where there is no excitation. The spatially periodic variation in the susceptibility acts as a diffraction grating that diffracts a portion of the probe pulse. The diffracted portion decays in a manner determined by the population and orientational dynamics of the sample. The first-order diffraction of the probe pulse from the grating is the transient grating signal's light field. The detected signal is the absolute value squared of the signal field.

In a pump–probe experiment, a pump pulse creates excited states, resulting in a reduction in the ground-state population (a bleach). After a delay τ, a probe pulse's transmission is measured. In comparison to the transmission with no pump, the probe's transmission is modified by the reduction in absorption that arises from the bleaching and amplification of the probe by simulated emission from the excited states. Although the ground-state and excited-state dynamics are not necessarily the same,[12] for our purposes here it is sufficient to take the time dependence of the two contributions to the signal to be identical. None of the issues addressed below is changed if the ground-state and excited-state dynamics differ. This transient change in transmission of the probe pulse in a pump–probe experiment can be viewed as a signal field created by the interactions of the pump and probe pulses with the sample propagating in the $\mathbf{k}_s=-\mathbf{k}_1+\mathbf{k}_1+\mathbf{k}_2$ direction, where $\mathbf{k}_1$ and $\mathbf{k}_2$ in this case are the directional vectors of the pump and the probe pulses, respectively. Following the sample, the signal is collinear with the probe pulse. The probe pulse acts as a local oscillator field and heterodynes with the signal field to yield the pump–probe signal.[23,24] The heterodyne detected nature of the signal in a pump–probe experiment is elaborated on a few paragraphs below. We henceforth treat the transient grating and pump–probe signal fields similarly, as both arising from the third-order material polarization of the sample.

We assume in this analysis that both orientational and population dynamics are slow compared with the pulse duration of the interacting light fields, permitting the use of delta functions to model the interacting light fields. With the pump pulse(s) having parallel polarization, the resultant signal field polarization, as a function of the polarization of the probe-pulse polarization, is

$$\vec{E}_{\mathrm{si}}(\tau,\theta_{\mathrm{pi}})=\mathbf{S}(\tau)\vec{E}_{\mathrm{pi}}(\theta_{\mathrm{pi}}), \tag{6}$$

where $\mathbf{S}(\tau)$ is the sample signal matrix that generates signal field $\vec{E}_{\mathrm{si}}(\tau,\theta_{\mathrm{pi}})$ immediately after the sample, given an incident probe field $\vec{E}_{\mathrm{pi}}(\theta_{\mathrm{pi}})$. $\vec{E}_{\mathrm{pi}}(\theta_{\mathrm{pi}})$ is the initial probe field immediately before the sample. Within the diagrammatic perturbation theory framework, $\vec{E}_{\mathrm{pi}}(\theta_{\mathrm{pi}})$ is unchanged by the sample. $\vec{E}_{\mathrm{si}}(\tau,\theta_{\mathrm{pi}})$ and $\vec{E}_{\mathrm{pi}}(\theta_{\mathrm{pi}})$ are the signal and the probe fields, respectively, that emerge from the sample before the influence of any subsequent optical elements. τ is the delay between the pump pulse(s) and the probe pulse. An equality sign is used in Eq. (6) instead of a proportionality sign to simplify the notation because we are interested in the relative amplitudes of the polarization components of the signal field, not in the absolute amplitude. Sample signal matrix $\mathbf{S}(\tau)$ can be written as

$$\mathbf{S}(\tau)=\begin{bmatrix} R_{\parallel}(\tau) & 0 \\ 0 & R_{\perp}(\tau) \end{bmatrix}, \tag{7}$$

where $R_{\parallel}(\tau)$ and $R_{\perp}(\tau)$ are the orientational response functions for the parallel and perpendicular components, respectively:

$$R_{\parallel}(\tau)=\tfrac{1}{3}\left[1+\tfrac{4}{5}C_2(\tau)\right]P(\tau), \tag{8}$$

$$R_{\perp}(\tau)=\tfrac{1}{3}\left[1-\tfrac{2}{5}C_2(\tau)\right]P(\tau). \tag{9}$$

$P(\tau)$ describes the excited-state population relaxation, and the orientational relaxation $C_2(\tau)=\langle P_2(\hat{\mu}(t)\cdot\hat{\mu}(0))\rangle$ is represented by the orientation autocorrelation function for the second-order Legendre polynomial (P_2) of the transitional dipole moment unit vector.[8,9] Cast in the language of diagrammatic perturbation theory, $R_{\parallel}$ and $R_{\perp}$ are, respectively, the third-order nonlinear tensorial polarization elements R_{XXXX} and R_{YYXX}.[9]

Detectors used for optical experiments measure the intensity of the impinging signal. For a pump–probe experiment we can view the measurement made by the detector as the heterodyne detection of the signal field ($\vec{E}_{\mathrm{sf}}^{\,*}$), with the probe beam providing the local oscillator field ($\vec{E}_{\mathrm{pf}}$).[23] $\vec{E}_{\mathrm{sf}}$ and $\vec{E}_{\mathrm{pf}}$ are, respectively, the final signal and probe fields after they have passed through all optical elements that come after the sample. Then the detected signal is[25]

$$S_{\mathrm{PP}}=2\,\mathrm{Re}(\vec{E}_{\mathrm{sf}}^{\,*}\cdot\vec{E}_{\mathrm{pf}}). \tag{10}$$

In contrast, the signal from a transient grating experiment is usually homodyne detected. The outgoing signal propagates in a unique direction, and it does not overlap the probe pulse spatially. Then the transient grating signal is the absolute square of the signal field:

$$S_{\mathrm{TG}}=\vec{E}_{\mathrm{sf}}^{\,*}\cdot\vec{E}_{\mathrm{sf}}. \tag{11}$$

3. MAGIC ANGLE EXPERIMENTS TO MEASURE POPULATION-RELAXATION DYNAMICS

One common use of polarization-selective spectroscopy is to study population dynamics following electronic or vibrational excitation of a sample of molecules that are also undergoing orientational relaxation. In a pump–probe experiment, if the probe pulse polarization is at the magic angle $\theta_{\mathrm{ma}}=54.7°$, the resultant probe signal as a function of delay time τ will not contain contributions from orientational dynamics, provided that the experiment is properly implemented. The time-dependent signal is purely due to the excited-population-state lifetime[1–3] or possibly

Table 1. Implementations That May Give Population-Only Dynamics for Pump–Probe and Transient Grating (TG) Experiments

Case	Optical Operator[a]	Signal Field, E_{sf}	Probe Field, E_{pf}	Population Only[b]	
				Pump–Probe	Transient Grating
A	$\mathbf{I}E_k(\theta_{ma})$	$\begin{bmatrix} R_{\parallel}(\tau)\cos\theta_{ma} \\ R_{\perp}(\tau)\sin\theta_{ma} \end{bmatrix}$	$\begin{bmatrix} \cos\theta_{ma} \\ \sin\theta_{ma} \end{bmatrix}$	Y	N
B	$\mathbf{M}E_k(\theta_{ma})$	$\begin{bmatrix} \exp(i\delta)R_{\parallel}(\tau)\cos\theta_{ma} \\ R_{\perp}(\tau)\sin\theta_{ma} \end{bmatrix}$	$\begin{bmatrix} \exp(i\delta)\cos\theta_{ma} \\ \sin\theta_{ma} \end{bmatrix}$	Y	N
C	$\mathbf{P}(\theta_{ma})E_k(\theta_{ma})$	$(R_{\parallel}\cos^2\theta_{ma}+R_{\perp}\sin^2\theta_{ma})\begin{bmatrix} \cos\theta_{ma} \\ \sin\theta_{ma} \end{bmatrix}$	$\begin{bmatrix} \cos\theta_{ma} \\ \sin\theta_{ma} \end{bmatrix}$	Y	Y
D	$\mathbf{MP}(\theta_{ma})E_k(\theta_{ma})$	$(R_{\parallel}\cos^2\theta_{ma}+R_{\perp}\sin^2\theta_{ma})\begin{bmatrix} \exp(i\delta)\cos\theta_{ma} \\ \sin\theta_{ma} \end{bmatrix}$	$\begin{bmatrix} \exp(i\delta)\cos\theta_{ma} \\ \sin\theta_{ma} \end{bmatrix}$	Y	Y
E	$\mathbf{P}(\theta_{ma})\mathbf{M}E_k(\theta_{ma})$	$[\exp(i\delta)R_{\parallel}\cos^2\theta_{ma}+R_{\perp}\sin^2\theta_{ma}]\begin{bmatrix} \cos\theta_{ma} \\ \sin\theta_{ma} \end{bmatrix}$	$[\exp(i\delta)\cos^2\theta_{ma}+\sin^2\theta_{ma}]\begin{bmatrix} \cos\theta_{ma} \\ \sin\theta_{ma} \end{bmatrix}$	N	N
F	$\mathbf{T}E_k(\theta_{ma})$	$\begin{bmatrix} \alpha R_{\parallel}(\tau)\cos\theta_{ma} \\ \beta R_{\perp}(\tau)\sin\theta_{ma} \end{bmatrix}$	$\begin{bmatrix} \alpha\cos\theta_{ma} \\ \beta\sin\theta_{ma} \end{bmatrix}$	N	N
G	$\mathbf{TMP}(\theta_{ma})E_k(\theta_{ma})$	$(R_{\parallel}\cos^2\theta_{ma}+R_{\perp}\sin^2\theta_{ma})\begin{bmatrix} \alpha\exp(i\delta)\cos\theta_{ma} \\ \beta\sin\theta_{ma} \end{bmatrix}$	$\begin{bmatrix} \alpha\exp(i\delta)\cos\theta_{ma} \\ \beta\sin\theta_{ma} \end{bmatrix}$	Y	Y
H	$\mathbf{P}(\theta_{ma})\mathbf{TM}E_k(\theta_{ma})$	$[\alpha\exp(i\delta)R_{\parallel}\cos^2\theta_{ma}+\beta R_{\perp}\sin^2\theta_{ma}]\begin{bmatrix} \cos\theta_{ma} \\ \sin\theta_{ma} \end{bmatrix}$	$[\alpha\exp(i\delta)\cos^2\theta_{ma}+\beta\sin^2\theta_{ma}]\begin{bmatrix} \cos\theta_{ma} \\ \sin\theta_{ma} \end{bmatrix}$	N	N
I	$\mathbf{P}(\theta_{ma})E_k(\theta_N)$	$(R_{\parallel}\cos\theta_N\cos\theta_{ma}+R_{\perp}\sin\theta_N\sin\theta_{ma})\begin{bmatrix} \cos\theta_{ma} \\ \sin\theta_{ma} \end{bmatrix}$	$(\cos\theta_N\cos\theta_{ma}+\sin\theta_N\sin\theta_{ma})\begin{bmatrix} \cos\theta_{ma} \\ \sin\theta_{ma} \end{bmatrix}$	N	N

[a] For the probe field, $E_k=E_{pi}$. For the signal field, $E_k=E_{si}=\mathbf{S}E_{pi}$, with $\mathbf{S}$ defined in Eq. (7).

[b] Y, yes; N, no.

to other processes, such as photochemistry,[12] that can affect the population of excited states. In practice, to perform the experiments one needs to place various optical elements along the beam path. These elements, as we show below, may or may not affect the polarization-sensitive signal measured. In this section we consider various cases that are likely to be encountered in setting up pump–probe or transient grating magic angle experiments. We analyze the experiments performed to determine whether they are indeed magic angle experiments that yield only population dynamics without contributions from orientational dynamics.

We consider various possible placements of optics. Column 2 of Table 1 lists the operators in the sequence of their placement (first element at the right) along the path of the signal after the sample cell for the various cases. Cases A–H are for a probe beam with its polarization fixed at the magic angle. In case I we consider instead a probe polarized at an angle other than the magic angle. For all cases A–I to be discussed, we assume that the impinging probe field is linearly polarized, i.e., that $\phi=0°$ in Eq. (2). We can ensure linear polarization by placing the polarizer (or half-wave plate) that is used to control the probe polarization immediately before the sample. The forms for final polarization of the signal and probe beams are evaluated and listed in columns 3 and 4, respectively, of Table 1. The heterodyne (pump–probe) and homodyne (transient grating) signals are evaluated in accordance with Eqs. (10) and (11), respectively. From the resultant expressions, we deduce whether the signal contains only excited-state population dynamics without an orientational dynamics component in it.

A population-dynamics-only signal will occur solely when the detected signal contains the terms of the parallel and perpendicular orientational response functions in the form

$$S(\tau) \propto R_{\parallel}(\tau)\cos^2\theta_{\mathrm{ma}} + R_{\perp}(\tau)\sin^2\theta_{\mathrm{ma}} = R_{\parallel}(\tau) + 2R_{\perp}(\tau) \propto P(\tau). \tag{12}$$

This form ensures that the two response functions [Eqs. (8) and (9)] are in the exact ratio such that the orientational contributions are canceled out. It does not matter whether the right-hand side of the first line of Eq. (12) is multiplied by a constant or raised to a power. Only population dynamics will be measured, so long as the result contains exactly this form and no other terms contain $R_{\parallel}$ and $R_{\perp}$. The presence or absence of the term in this form is listed as a Y (yes) or N (no) entry in the last two columns of Table 1 for the pump–probe and transient grating experiments.

To obtain the results discussed below, we use Table 1 in the following manner: The columns labeled Signal Field and Probe Field give the forms for the final fields ($\vec{E}_{\mathrm{sf}}$ and $\vec{E}_{\mathrm{pf}}$) after the initial fields ($\vec{E}_{\mathrm{si}}$ and $\vec{E}_{\mathrm{pi}}$) have passed through all relevant optical elements. The fields are given as column vectors. We obtain the final signal field and probe field by operating the string of operators, one for each optical element, on the initial fields, $\vec{E}_{\mathrm{si}}$ and $\vec{E}_{\mathrm{pi}}$, with $\vec{E}_{\mathrm{si}} = \mathbf{S}\vec{E}_{\mathrm{pi}}$ [see Eq. (7)]. Then the pump–probe and transient grating signals are given by Eqs. (10) and (11). The last two columns in Table 1 tell whether the signals produced in fact are magic angle signals that give only the population dynamics, that is, where the signals meet the condition given in relation (12).

Case A

Case A occurs if there are no optics between the sample and the detector; i.e., only the identity operator,

$$\mathbf{I} = \begin{bmatrix} 1 & 0 \\ 0 & 1 \end{bmatrix}, \tag{13}$$

operates on the initial fields. The measured pump–probe signal as a function of delay τ is

$$S_{\mathrm{PP}}(\tau) \propto R_{\parallel}(\tau)\cos^2\theta_{\mathrm{ma}} + R_{\perp}(\tau)\sin^2\theta_{\mathrm{ma}}, \tag{14}$$

which gives a signal containing purely population dynamics [relation (12)].

For a transient grating experiment, the homodyne detection yields a signal

$$S_{\mathrm{TG}}(\tau) \propto R_{\parallel}{}^2(\tau)\cos^2\theta_{\mathrm{ma}} + R_{\perp}{}^2(\tau)\sin^2\theta_{\mathrm{ma}}. \tag{15}$$

As can be seen, the resultant value is not relation (12) multiplied by a constant or raised to a power. Hence a homodyne detected transient grating signal produced from a probe (third) pulse that is set at the magic angle from the pump (first and second) pulses does not yield a purely population-dynamics signal in the simplest situation in which there are no other optical elements after the sample.

Case B

In practice, mirrors are needed to direct the signal from the sample to the detector. Reflection from a metal mirror introduces a phase shift that is different for S and P polarization. Because a magic angle probe pulse produces signal pulses (transmitted signal for pump–probe and diffracted signal pulse for a transient grating) that are neither purely S nor purely P polarized, the reflection from the metallic surface will result in elliptically polarized light. In the signal and probe fields given in Table 1 the ellipticity appears as the phase factor, $\exp(i\delta)$. For the pump–probe experiment the scalar product of the complex conjugate of the signal field and the probe field is taken [Eq. (10)], and the phase factors are eliminated. For the transient grating experiment the scalar product of the complex conjugate of the signal field and the signal field is taken [Eq. (11)], and again the phase factors are eliminated. The results show that the phase shifts introduced by a mirror or a number of mirrors have no effect on the nature of the signal. Both pump–probe (heterodyne) and transient grating (homodyne) experiments give the same result as does case A.

Case C

We next consider a polarizer set at magic angle θ_{ma} immediately after the sample, with no mirrors or other optical elements after the sample other than the polarizer. The resultant final signal field after the signal has gone through the polarizer is

$$\vec{E}_{\mathrm{sf}} = \mathbf{P}(\theta_{\mathrm{ma}})\vec{E}_{\mathrm{si}}(\tau, \theta_{\mathrm{ma}}) = (R_{\parallel}\cos^2\theta_{\mathrm{ma}} + R_{\perp}\sin^2\theta_{\mathrm{ma}}) \times \begin{bmatrix} \cos\theta_{\mathrm{ma}} \\ \sin\theta_{\mathrm{ma}} \end{bmatrix}. \tag{16}$$

The polarizer has no effect on the probe pulse, as the probe pulse is already polarized at the magic angle. The resultant heterodyne signal [Eq. (10)] is $S_{\mathrm{PP}} \propto (R_{\parallel}\cos^2\theta_{\mathrm{ma}} + R_{\perp}\sin^2\theta_{\mathrm{ma}})$, the desired population dynamics. The transient grating signal [Eq. (11)] is

$$S_{\mathrm{TG}}(\tau) \propto [R_{\parallel}(\tau)\cos^2\theta_{\mathrm{ma}} + R_{\perp}(\tau)\sin^2\theta_{\mathrm{ma}}]^2. \tag{17}$$

When a polarizer is placed at the magic angle after the sample, the transient grating signal yields pure population dynamics, in contrast to the results for case A. Observe that in the signal field of relation (16), the orientational-dynamics-free term [relation (12)] is already formed and falls outside the polarization vector. Hence any subsequent distortion and manipulation of the polarization of the signal field will not affect the orientational-dynamics-free term. This useful fact will manifest itself again in case D as well as in others that we are considering.

Case D

A more realistic setup than case C is the placement of the polarizer (adjusted to the magic angle) immediately after the sample and followed by mirrors to direct the signal or probe beams or both to the detector. Again, we consider the ellipticity resulting from reflections off the metallic mirrors. The analysis shows that the result is the same as in case C. From Table 1, signal and probe fields contain phase factors that vanish when the scalar product between a field and a complex-conjugate field is taken. Both the pump–probe and transient grating experiments give orientational-dynamics-free signals. This is to be expected, as was pointed out for case C, because any ma-

nipulation of the polarization after the analyzing polarizer does not affect the orientational-dynamics-free term in the signal.

In light of the analysis of cases B–D, it should be pointed out that in some reports in the literature in which transient grating experiments are employed there is no attempt to draw a difference, as far as the we can tell, between a transient grating experiment that is performed with or without an analyzing polarizer adjusted to the magic angle.[4,5]

Case E

Although the situations described for cases C and D permit the use of a magic angle transient grating experiment, it is important to consider the effect of placing one or more mirrors after the sample but before a polarizer set at the magic angle for both the transient grating and pump–probe experiments. As can be seen from the expressions listed in Table 1, neither pump–probe nor transient grating signals give pure population dynamics. One or more mirrors introduce a phase shift, δ, between the two polarization components of the fields. The pump–probe signal is given by

$$S_{\mathrm{PP}}(\tau) \propto R_{\parallel}(\tau)(1 + 2\cos\delta) + 2R_{\perp}(\tau)(\cos\delta + 2). \quad (18)$$

Depending on the value of δ, the relative contributions of $R_{\parallel}(\tau)$ and $R_{\perp}(\tau)$ to the measured signal vary.

To illustrate how the measured pump–probe signal deviates from the magic angle condition as a function of ellipticity, we define a quantity Q that is the absolute value of the ratio of the orientational-dynamics amplitude to the population-dynamics-only amplitude. For instance, the Q values for the measurement of pure $R_{\parallel}(\tau)$ signal and pure $R_{\perp}(\tau)$ signal [Eqs. (8) and (9)] are 0.8 and 0.4, respectively, whereas a signal that is due to pure population dynamics has a $Q=0$ value. Q is plotted in Fig. 2 as a function of phase shift δ. For a phase shift of nearly 180°, the

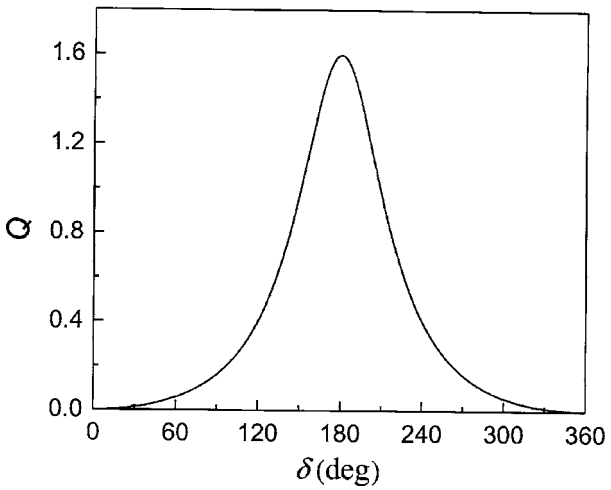

Fig. 2. Q is the absolute value of the ratio of the amplitude of the orientational-dynamics component to the amplitude of the population-dynamics component that is measured in a pump–probe experiment under the conditions presented for case E. Q, calculated from relation (18), is plotted as a function of δ, the phase shift introduced between the S and P components by reflection from one or several mirrors. A signal time dependence that arises from purely population dynamics occurs for $Q=0$.

Q value is 1.6. In this situation the measured signal contains twice the orientational dynamics component than in a nonmagic angle experiment, which just measures $R_{\parallel}(\tau)$. The phase-shift value mentioned in Section 2 for a single reflection from a silver surface of a beam in the visible is $\delta=26°$ at 500 nm. In this case it takes only four or five mirrors before a supposedly magic angle experiment is degraded to the point that a signal is obtained with similar orientational-dynamics contamination as in an experiment measuring only $R_{\perp}(\tau)$. At mid-infrared wavelengths the problem is less serious but may still give a measurable difference, depending on the population relaxation $P(\tau)$ and orientational relaxation $C_2(\tau)$.

The transient grating signal for this case is described by the equation

$$S_{\mathrm{TG}}(\tau) \propto R_{\parallel}^{\,2}(\tau) + 4R_{\perp}^{\,2}(\tau) + 4\cos\delta R_{\parallel}(\tau)R_{\perp}(\tau). \quad (19)$$

As can be seen, the transient grating signal also does not measure solely the population dynamics.

Case F

In case F and in the next few cases we consider the inclusion of optics in the experimental setup that does not have the same effect on S and P polarizations. Such optics are, for example, a diffraction grating and a beam splitter. In many situations, one conducts wavelength-selective experiments by passing the signal through a monochromator. Ultrafast spectroscopy of vibrational systems uses pulses with broad bandwidths that span the 0–1 as well as the 1–2 transition. Hence frequency-resolved detection of the signal is often used to separate the 0–1 and 1–2 transitions.[14] One can achieve frequency resolution following broadband pumping by sending the signal and probe beams through a monochromator before the detector. The polarization-selective optics in this case is a diffraction grating in the monochromator. Diffraction gratings, in general, diffract the S and P polarization of the incident light with different efficiencies. The resultant pump–probe signal is

$$\begin{aligned} S_{\mathrm{PP}}(\tau) &\propto \alpha^2 R_{\parallel}(\tau)\cos^2\theta_{\mathrm{ma}} + \beta^2 R_{\perp}(\tau)\sin^2\theta_{\mathrm{ma}} \\ &= \alpha^2 R_{\parallel}(\tau) + 2\beta^2 R_{\perp}(\tau) \end{aligned} \quad (20)$$

[see Eq. (5)]. Unless $\alpha=\beta$, i.e., unless the diffraction grating has equal diffraction efficiency for both polarizations, the resultant signal will not reflect the population-only dynamics that is obtained from a magic angle experiment in the absence of a monochromator. It is theoretically possible to adjust incoming probe angle θ_p to compensate for the efficiency discrepancy by satisfying the relation

$$2\alpha^2\cos^2\theta_p = \beta^2\sin^2\theta_p. \quad (21)$$

Generally, the efficiency difference for the two polarizations is a function of wavelength, and the angle would need to be determined and adjusted for each wavelength. This compensation scheme will not be applicable if an array detector (CCD or IR array) is used to detect the signal simultaneously over a broad spectral range. For the transient grating experiment, the signal does not contain solely population dynamics. In the absence of the monochromator (case A), the transient grating experiment with the probe at the magic angle does not measure population

dynamics only. Adding a monochromator does not improve the situation, and there is no angle θ_p that fixes the problem, even for a single detection frequency. The need for care in making measurements through a monochromator has not always been recognized.[12]

Case G

We can eliminate the problems encountered in case F by placing a polarizer set at the magic angle immediately after the sample. We also include the effects of reflections off metallic mirrors in this case. The resultant heterodyne signal gives pure population dynamics:

$$S_{\mathrm{PP}}(\tau) \propto (R_{\parallel} \cos^2 \theta_{\mathrm{ma}} + R_{\perp} \sin^2 \theta_{\mathrm{ma}})(\alpha^2 \cos^2 \theta_{\mathrm{ma}} + \beta^2 \sin^2 \theta_{\mathrm{ma}}). \tag{22}$$

Similarly, the transient grating signal contains only the relevant population-dynamics component. This is in accord with case C, in which it was shown that changes in the polarization of the signal light field after the polarizer do not affect the nature of the signal. If mirrors are included in the setup, as they are in the calculation, it is necessary to place the polarizer immediately after the sample before any mirrors to prevent occurrence of the problem delineated in case E.

Case H

To complete the discussion of the polarization-selective optics, we considered placing the polarizer after the monochromator. As can be seen for this case from Table 1, for both the pump–probe and transient grating experiments the resultant signals do not give pure population dynamics.

Case I

We include here one more situation that might be misconstrued to be the equivalent of a true magic angle experiment. We consider the case in which the probe's polarization is set at an angle θ_N other than the magic angle but a polarizer placed after the sample is set at the magic angle. This case is similar to the situation in case C, except for the incoming probe polarization. It can be seen from the entires in Table 1 that the resultant signals do not yield solely population dynamics. Therefore setting the analyzing polarizer to the magic angle does not guarantee magic angle detection. However, we note here as an academic exercise that, given an analyzing polarizer set at an angle θ_M, there will be a probe polarization angle θ_N that yields that magic angle condition if the following condition is satisfied:

$$\tan \theta_M \tan \theta_N = 2. \tag{23}$$

4. POLARIZATION-SELECTIVE EXPERIMENTS TO MEASURE ORIENTATIONAL DYNAMICS

One of the most useful applications of polarization spectroscopy is the measurement of molecular orientational dynamics in liquids. The orientational dynamics are obtained from two sets of experiments that determine $R_{\parallel}(\tau)$ and $R_{\perp}(\tau)$ separately. Then the orientational correlation function for a dipole transition, $C_2(\tau)$, is related to $R_{\parallel}(\tau)$ and $R_{\perp}(\tau)$ by the expression

$$\frac{2}{5} C_2(\tau) = \frac{R_{\parallel}(\tau) - R_{\perp}(\tau)}{R_{\parallel}(\tau) + 2R_{\perp}(\tau)}. \tag{24}$$

Measuring $R_{\parallel}(\tau)$ and $R_{\perp}(\tau)$ can also provide the population-only dynamics according to relation (12). One way to determine $R_{\parallel}(\tau)$ and $R_{\perp}(\tau)$ is to use a probe pulse with a polarization at angle θ_{pi} other than parallel or perpendicular (usually 45°). An analyzing polarizer before the detector set at angle $\theta_A = 0°$ [90°] will select the parallel [perpendicular] component and measure $R_{\parallel}(\tau)$ [$R_{\perp}(\tau)$] only.[6] The question arises as to whether the position of the polarizer along the optical path will affect the nature of the signal that is detected. Consider the situation like that of case H in Section 2. To measure $R_{\parallel}(\tau)$ we set the analyzing polarizer at $\theta_A = 0°$. The resultant signal field is

$$\vec{E}_{\mathrm{sf}} = \mathbf{P}(\theta_A = 0°)\mathbf{T}\mathbf{M}\boldsymbol{E}_{\mathrm{si}}(\tau, \theta_{\mathrm{pi}}) = \begin{bmatrix} \alpha \exp(i\delta) R_{\parallel}(\tau) \cos \theta_A \\ 0 \end{bmatrix}, \tag{25}$$

and the resultant probe field is

$$\vec{E}_{\mathrm{pf}} = \mathbf{P}(\theta_A = 0°)\mathbf{T}\mathbf{M}\boldsymbol{E}_{\mathrm{si}}(\tau, \theta_{\mathrm{pi}}) = \begin{bmatrix} \alpha \exp(i\delta) \cos \theta_A \\ 0 \end{bmatrix}. \tag{26}$$

Both heterodyne (pump–probe) and homodyne (transient grating) detection of the signal yields a clean measurement of the time dependence of $R_{\parallel}(\tau)$. The same holds true for the measurement of the time dependence of $R_{\perp}(\tau)$ with the analyzing polarizer set at $\theta_A = 90°$. It is important to recognize that, for the pump–probe experiment, $R_{\parallel}(\tau)$ and $R_{\perp}(\tau)$ are multiplied by the time-independent constants $\alpha^2 \cos^2 \theta_A$ and $\beta^2 \cos^2 \theta_A$, respectively [Eq. (5)]. To use Eq. (24) we normalize out these factors by measuring the amplitudes of the probe with the detector in the absence of a signal with the polarizer set to parallel and to perpendicular. The required amplitudes can be measured either with the pump blocked or with delay τ set before $\tau = 0$. For transient grating experiments, ${R_{\parallel}}^2(\tau)$ and ${R_{\perp}}^2(\tau)$ are measured. Then the square root of these quantities must be taken before we use Eq. (24).

For the detection to be clean, the optical elements before the polarizer cannot mix the parallel and perpendicular components of the light field. This condition is equivalent to the statement that the off-diagonal elements of the operator matrices involved must be zero. This condition is fulfilled for the analyzing polarizer adjusted to $\theta_A = 0°$, 90°, the angles needed to detect $R_{\parallel}(\tau)$ and $R_{\perp}(\tau)$, respectively. The same condition of having only diagonal elements also guarantees that the operator matrix of the analyzing polarizers adjusted to $\theta_A = 0°$, 90°, $\mathbf{P}(\theta_A = 0°)$, and $\mathbf{P}(\theta_A = 90°)$ commutes with the operators $\mathbf{M}$ and $\mathbf{T}$, which similarly have only diagonal elements. Therefore, to obtain the correct time dependence of $R_{\parallel}(\tau)$ or $R_{\perp}(\tau)$ we can place the polarizer anywhere along the beam path.

Optics such as mirrors or a diffraction grating, placed before or after the polarizer, will not change the measured time dependence.

5. CONCLUDING REMARKS

Using Jones matrix calculus, we have analyzed the type of signal measured by polarization spectroscopies for various realistic experimental situations. The polarization spectroscopies analyzed are pump–probe and transient grating experiments designed to recover both the orientational and the population dynamics of a sample. For magic angle experiments, a transient grating experiment will yield a pure population-dynamics signal only if there is an analyzing polarizer placed immediately after the sample set at the magic angle. Without the analyzing polarizer, the signal will be contaminated by contributions from orientational dynamics. Such is not the case for magic angle pump–probe experiments in which an analyzing polarizer after the sample is not required if there are no polarization-selective optics, such as a diffraction grating, between the sample and the detector. However, for a pump–probe experiment with polarization-selective optics in the optical path following the sample, an analyzing polarizer at the magic angle must be used, and it is essential that the polarizer be placed immediately after the sample. For experiments that measure orientational relaxation as well as population relaxation by separately measuring the orientational response function $R_{\parallel}(\tau)$ and $R_{\perp}(\tau)$, the requirements are not so stringent. The position along the beam path of the analyzing polarizer following the sample is not critical for obtaining clean measurements of the time dependence of $R_{\parallel}(\tau)$ and $R_{\perp}(\tau)$.

We have provided a straightforward and rigorous framework in which to analyze and determine how effective a particular implementation of a polarization-selective spectroscopy experiment is for measuring the desired quantity. Although we have treated only certain specific experimental situations, the method is general. The forms of the Jones matrices that have been presented for various optical components can be used to investigate any combination of optical components. For example, while we determined the influence of the phase shift between S and P polarization that is introduced by reflection from a mirror, we did not explicitly consider the fact that mirrors do not reflect S and P polarization identically. If there are many mirrors in the optical path, the difference in reflectivity can become significant. The difference in mirror reflectivity can be treated by use of the **T** matrix [Eq. (5)] for polarization-selective optical elements. The approach presented here will help experimentalists to avoid the types of pitfall that have been illustrated above.

ACKNOWLEDGMENTS

This study was supported by the U.S. Department of Energy (grant DE-FG03-84ER13251) and the National Science Foundation (grant DMR-0332692).

H.-S. Tan's e-mail address is tanhs@alumni.princeton.edu. M. D. Fayer's e-mail address is fayer@stanford.edu.

*Permanent address, School of Physical and Mathematical Sciences, Nanyang Technological University, 1 Nanyang Walk, Singapore 637616.

REFERENCES

1. H. E. Lessing and A. V. Jena, "Separation of rotational diffusion and level kinetics in transient absorption spectroscopy," Chem. Phys. Lett. **42**, 213–217 (1976).
2. G. R. Fleming, *Chemical Applications of Ultrafast Spectroscopy* (Oxford U. Press, 1986).
3. H. Graener, G. Seifert, and A. Laubereau, "Direct observation of rotational relaxation-times by time-resolved infrared-spectroscopy," Chem. Phys. Lett. **172**, 435–439 (1990).
4. A. Von Jena and H. E. Lessing, "Theory of laser-induced amplitude and phase gratings including photoselection, orientational relaxation and population-kinetics," Opt. Quantum Electron. **11**, 419–439 (1979).
5. R. S. Moog, M. D. Ediger, S. G. Boxer, and M. D. Fayer, "Viscosity dependence of the rotational reorientation of Rhodamine-B in mono-alcohol and poly-alcohol—picosecond transient grating experiments," J. Phys. Chem. **86**, 4694–4700 (1982).
6. A. B. Myers and R. M. Hochstrasser, "Comparison of 4-wave-mixing techniques for studying orientational relaxation," IEEE J. Quantum Electron. **22**, 1482–1492 (1986).
7. O. Teschke, E. P. Ippen, and G. R. Holtom, "Picosecond dynamics of singlet excited-state of *trans*-stilbene and *cis*-stilbene," Chem. Phys. Lett. **52**, 233–235 (1977).
8. T. Tao, "Time-dependent fluorescence depolarization and Brownian rotational diffusion coefficients of macromolecules," Biopolymers **8**, 609–632 (1969).
9. A. Tokmakoff, "Orientational correlation functions and polarization selectivity for nonlinear spectroscopy of isotropic media. 1. Third order," J. Chem. Phys. **105**, 1–12 (1996).
10. Q. Zhong, A. P. Baronavski, and J. C. Owrutsky, "Reorientation and vibrational energy relaxation of pseudohalide ions confined in reverse micelle water pools," J. Chem. Phys. **119**, 9171–9177 (2003).
11. H. Maekawa, K. Ohta, and K. Tominaga, "Vibrational population relaxation of the —N═C═N—antisymmetric stretching mode of carbodiimide studied by the infrared transient grating method," J. Phys. Chem. A **108**, 9484–9491 (2004).
12. T. Steinel, J. B. Asbury, J. Zheng, and M. D. Fayer, "Watching hydrogen bonds break: a transient absorption study of water," J. Phys. Chem. A **108**, 10,957–10,964 (2004).
13. G. M. Sando, Q. Zhong, and J. C. Owrutsky, "Vibrational and rotational dynamics of cyanoferrates in solution," J. Chem. Phys. **121**, 2158–2168 (2004).
14. H.-S. Tan, I. R. Piletic, and M. D. Fayer, "Orientational dynamics of water confined on a nanometer length scale in reverse micelles," J. Chem. Phys. **122**, 174501 (2005).
15. R. C. Jones, "A new calculus for the treatment of optical systems. I. Description and discussion of the calculus," J. Opt. Soc. Am. **31**, 488–493 (1941).
16. E. Hecht, *Optics*, 4th ed. (Addison-Wesley, 2002).
17. D. Waldeck, A. J. Cross, D. B. Mcdonald, and G. R. Fleming, "Picosecond pulse induced transient molecular birefringence and dichroism," J. Chem. Phys. **74**, 3381–3387 (1981).
18. X. L. Xie and J. D. Simon, "Picosecond circular-dichroism spectroscopy—a Jones matrix analysis," J. Opt. Soc. Am. B **7**, 1673–1684 (1990).
19. M. J. Feldstein, P. Vohringer, and N. F. Scherer, "Rapid-scan pump-probe spectroscopy with high time and wave-

number resolution—optical-Kerr-effect measurements of neat liquids," J. Opt. Soc. Am. B **12**, 1500–1510 (1995).
20. M. Born and E. Wolf, *Principles of Optics*, 7th ed. (Cambridge U. Press, 1999).
21. L. H. Johnston, "Broad-band polarization rotator for infared," Appl. Opt. **16**, 1082–1084 (1977).
22. C. Palmer, *Diffraction Grating Handbook*, 4th ed. (Richardson Grating Laboratory, Rochester, N.Y., 2000).
23. S. Mukamel, *Principles of Nonlinear Optical Spectroscopy* (Oxford U. Press, 1995).
24. J. E. Rothenberg, "Self-induced heterodyne—the interaction of a frequency-swept pulse with a resonant system," IEEE J. Quantum Electron. **22**, 174–181 (1986).
25. M. D. Levenson, *Introduction to Nonlinear Laser Spectroscopy* (Academic, 1982).